

Guest Recognition in a Partially Bridged Deep Cavitand

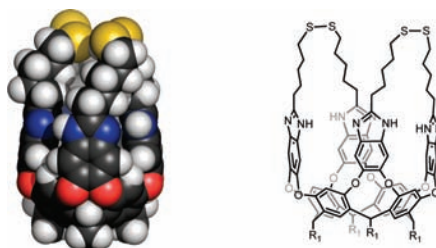
Eric Busseron and Julius Rebek, Jr.*

The Skaggs Institute for Chemical Biology and Department of Chemistry, The Scripps Research Institute, 10550 North Torrey Pines Road, La Jolla, California 92037, United States

jrebek@scripps.edu

Received August 20, 2010

ABSTRACT



The synthesis of a new deep cavitand partially bridged via disulfide bonds is described. Its thermodynamic and kinetic complexation parameters are compared with those of an unbridged analogue. The disulfide bridges cause deviations in ΔH and ΔS but result in only small differences in ΔG of complexation. The bridges increase the activation barrier for guest dissociation and lead to complexes with enhanced kinetic stability.

Deep cavitands are synthetic receptors that provide modern vehicles for molecular recognition in physical organic and analytical chemistry. The vase-like shape of deep cavitands derived from resorcin[4]arene can be maintained by a seam of cooperative intramolecular hydrogen bonds present on the upper rim of the molecule,¹ by physicochemical conditions (temperature, pH),² or even through covalent bridges.³ The dynamic properties of the latter led us to consider the effects of extended covalent bridges connected in pairs on a deep

cavitand⁴ and we report here the synthesis and characterization of such a system. The cavitand is partially bridged using disulfide bonds that offer an alternate mean of guest control and new sites for attachment to solid surfaces.

The starting point is the well-known octanitro cavitand **1** bearing C₁₁ alkyl “feet”.^{1c} Reduction of the nitro groups with SnCl₂·2H₂O in a mixture of EtOH and concd HCl at reflux gave the corresponding octaamine hydrochloride.

This intermediate was directly condensed with the thioester imidate **2**⁵ in dry ethanol at reflux to afford the tetrathioester cavitand **3**. The yield of purified material was 63% over two steps. The desired partially bridged deep cavitand **5** could then be obtained from **3** by two different pathways (Scheme 1).

In the first, the cleavage of the thioacetate groups was accomplished with excess LiAlH₄ to prevent any oxidation to disulfide bonds. After quenching with AcOH and purifica-

(1) (a) Lledo, A.; Rebek, J., Jr. *Chem. Commun.* **2010**, 46, 1637. (b) Mann, E.; Rebek, J., Jr. *Tetrahedron* **2008**, 64, 8484. (c) Far, A. R.; Shivanyuk, A.; Rebek, J., Jr. *J. Am. Chem. Soc.* **2002**, 124, 2854. (d) Rudkevich, D. M.; Hilmersson, G.; Rebek, J., Jr. *J. Am. Chem. Soc.* **1998**, 120, 12216. (e) Rudkevich, D. M.; Hilmersson, G.; Rebek, J., Jr. *J. Am. Chem. Soc.* **1997**, 119, 9911.

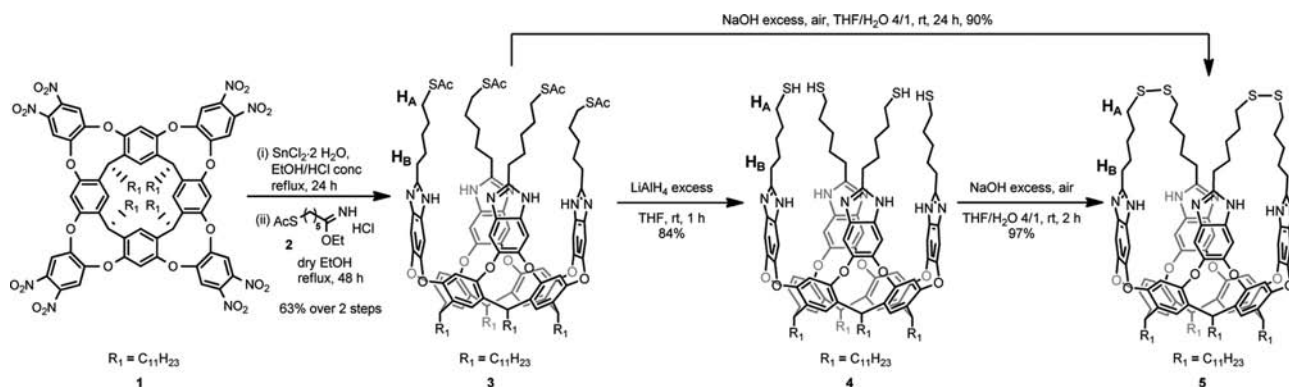
(2) (a) Shirtcliff, L. D.; Xu, H.; Diederich, F. *Eur. J. Org. Chem.* **2010**, 846. (b) Azov, V. A.; Schlegel, A.; Diederich, F. *Angew. Chem., Int. Ed.* **2005**, 44, 4635. (c) Moran, J. R.; Ericson, J. L.; Dalcanale, E.; Bryant, J. A.; Knobler, C. B.; Cram, D. J. *J. Am. Chem. Soc.* **1991**, 113, 5707. (d) Moran, J. R.; Karbach, S.; Cram, D. J. *J. Am. Chem. Soc.* **1982**, 104, 5826.

(3) (a) Gottschalk, T.; Jarowski, P. D.; Diederich, F. *Tetrahedron* **2008**, 64, 8307. (b) Gottschalk, T.; Jaun, B.; Diederich, F. *Angew. Chem., Int. Ed.* **2007**, 46, 260. (c) Gibb, C. L. D.; Sundaresan, A. K.; Ramamurthy, V.; Gibb, B. C. *J. Am. Chem. Soc.* **2008**, 130, 4069. (d) Gibb, C. L. D.; Gibb, B. C. *J. Am. Chem. Soc.* **2004**, 126, 11408. (e) Laughrey, Z. R.; Gibb, C. L. D.; Senechal, T.; Gibb, B. C. *Chem.—Eur. J.* **2003**, 9, 130.

(4) Some examples with calixarenes have been described: (a) Rudkevich, Y.; Rudkevich, V.; Klautzsch, F.; Schalley, C. A.; Böhrer, V. *Angew. Chem., Int. Ed.* **2009**, 48, 3867. (b) Lim, C. W.; Hong, J.-I. *Tetrahedron Lett.* **2000**, 41, 3113.

(5) See the Supporting Information.

Scheme 1. Synthesis of the Partially Bridged Deep Cavitant **5**



tion, the tetrathiol cavitant **4** was obtained in 84% yield. Air oxidation of **4** (2 mM) was carried out in a mixture of THF/H₂O (4/1)⁶ and excess NaOH^{6,7} with vigorous stirring for 2 h in open air. Neutralization with AcOH and purification gave compound **5** in 97% yield. Alternatively, a one-step approach can be used for the cleavage of the thioacetate groups of **3** and air oxidation of thiols in situ, using NaOH. After 24 h of vigorous stirring and workup as before, the same cavitant **5** was obtained in 90% yield.⁸

The ¹H NMR spectrum of cavitant **5** is compared with **4** in Figure 1. First, no trace of thiol remained in compound **5**

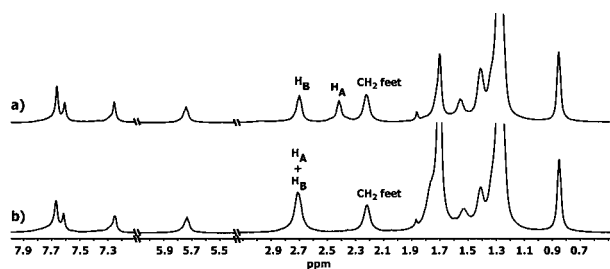


Figure 1. Partial ¹H NMR spectra (THF-*d*₈/D₂O 9/1, 300 K) of (a) cavitant **4** and (b) cavitant **5** from the stepwise approach. The lettering corresponds to the hydrogen assignments in Scheme 1.

(no CH₂SH signal between 2.53–2.34 ppm) showing that all thiols have been fully oxidized. Second, the chemical shift of hydrogens H_A ($\delta_{H_A} = 2.88\text{--}2.59$ ppm, broad singlet, THF-*d*₈/D₂O 9/1) is in good accord with that of the corresponding hydrogens in dibutyl disulfide ($\delta_{CH_2SS} = 2.66$ ppm) in the same mixture of deuterated solvents.⁵ Finally, the HRMS-ESI spectrum showed only the expected mass of **5**, and the MALDI-TOF spectrum showed no trace of oligomeric species.

(6) Schramm, M. P.; Hooley, R. J.; Rebek, J., Jr. *J. Am. Chem. Soc.* **2007**, *129*, 9773.

(7) (a) Singh, D.; Galetto, F. Z.; Soares, L. C.; Rodrigues, O. E. D.; Braga, A. L. *Eur. J. Org. Chem.* **2010**, 2661. (b) Wallace, T. J.; Schriesheim, A.; Bartok, W. *J. Org. Chem.* **1963**, *28*, 1311.

(8) Nevertheless, a minor unknown impurity is present in the ¹H NMR spectrum; see the Supporting Information.

The structure of **5** is modeled in Figure 2a, along with the isomer in which the disulfides span opposite walls in Figure 2b. The latter - a carcerand⁹ - while structurally feasible, is inconsistent with the kinetic behavior of guests described below.

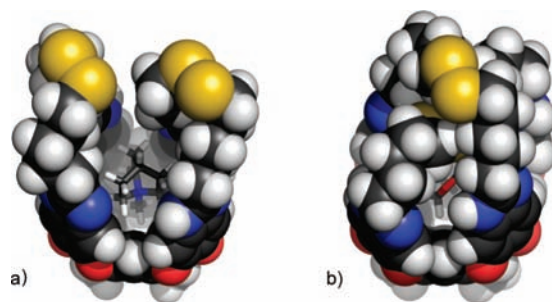


Figure 2. Energy-minimized structures (Spartan, PM3) of (a) cavitant **5** with a *N*-methylquinuclidinium **8** and (b) carcerand in which the disulfides span opposite walls, with a THF molecule inside the cavity.

The influence of the two covalent bridges on the recognition properties was determined by comparison of thermodynamic and kinetic complexation parameters of **5** vs the unbridged cavitant **3** for a series of guests (Figure 3). The parameters K_a and ΔG in Table 1 were determined by ¹H NMR at 300 K in DMSO-*d*₆. Neutral guests **6a** and **6b**

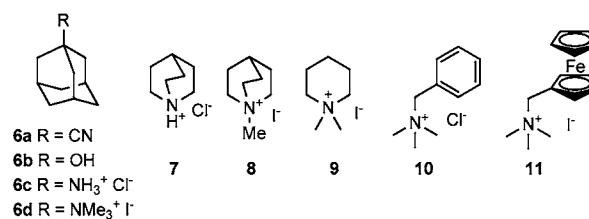


Figure 3. Guests used for the recognition studies in DMSO-*d*₆ with both cavitants **3** and **5**.

Table 1. Thermodynamic Parameters K_a and ΔG for Cavitands **3** and **5** with Guests **6a–d** and **7–11** Determined by ^1H NMR in $\text{DMSO-}d_6$ at 300 K^a

guests	K_a^b (M^{-1})		ΔG (kcal mol^{-1})		$\Delta\Delta G$ (kcal mol^{-1}) = $\Delta G(\mathbf{5}) - \Delta G(\mathbf{3})$
	3	5	3	5	
6a	<5	<5			
6b	<5	<5			
6c	n.d. ^c	n.d. ^c			
6d^d	697	1612	-3.9	-4.4	-0.5
7	<5	<5			
8	1790	2817	-4.5	-4.7	-0.2
9^d	498	974	-3.7	-4.1	-0.4
10	112	132	-2.8	-2.9	-0.1
11	n.d. ^c	n.d. ^c			

^a Cavitand concentration 1–3 mM. ^b Errors are within 10% from an average of at least three experiments. ^c Bound guest was not detected on ^1H NMR spectrum, even with addition of a large excess of guest. ^d Reported values of K_a and ΔG were obtained from van't Hoff plots (see Figure 4) and are similar to the ones obtained by ^1H NMR experiments at 300 K.

showed very low association constants ($K_a < 5 \text{ M}^{-1}$) for both cavitands in this competing solvent. Guests offering cation- π interactions were tested, but neither cavitand bound the primary ammonium **6c**. For the tertiary ammonium guest **7**, some binding was detected, but the corresponding association constant was very low ($K_a < 5 \text{ M}^{-1}$) with either cavitand. According to the ^1H NMR and ROESY experiments, the methine hydrogen of the guest is positioned deep in the cavity; accordingly, the tertiary ammonium, near the upper rim, cannot interact significantly with the aromatics of the cavitand.

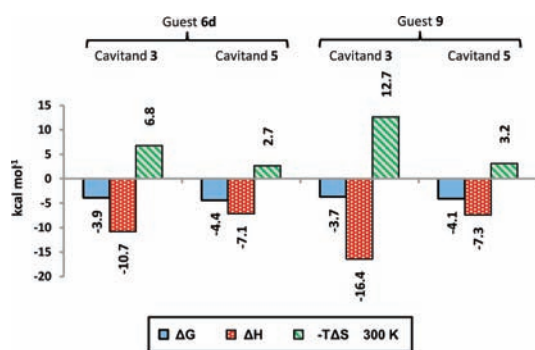


Figure 4. Values of ΔG , ΔH , and $-T\Delta S$ at 300 K extracted from van't Hoff plots of guests **6d** and **9** with both cavitands **3** and **5** in $\text{DMSO-}d_6$.

In contrast, a series of quaternary ammonium guests **6d**, **8**, **9**, and **10** showed good affinity for both cavitands. NOESY experiments indicated deeply positioned ammonium functions for all of these guests. The increase in association constants with the degree of alkylation of the ammonium

(9) Cram, D. J.; Cram, J. M. *Container Molecules and Their Guests*; Royal Society of Chemistry: Cambridge, 1994.

moiety, previously observed in water,¹⁰ was mainly attributed to a solvation effect. In DMSO , primary ammoniums are better solvated than secondary ones and so on.¹¹ Consequently, it is more energetically costly to fully desolvate a tertiary ammonium prior to its entry in the cavity than a quaternary one; this correctly predicts a lower K_a for guest **7** than **8**, if not the specific orientation of **7**. And guest **8** fits into the bottom of the cavity better than does **7**, so shape complementarity also contributes. Nevertheless, the difference in counterions of the two guests must also be considered.¹²

Finally, guest **11**, bearing a ferrocene group, does not form kinetically stable complexes with either cavitand in spite of its quaternary ammonium. It is likely that the shape and bulkiness of the ferrocene prevent the quaternary ammonium from penetrating deep into the cavity.

The association constants are consistently higher with **5** than with **3** for all guests **6d** and **8–10**. The calculation of ΔG from K_a values at 300 K was used to determine the $\Delta\Delta G$ values: these differences are quite small and vary from -0.1 to -0.5 kcal mol^{-1} .

In addition, van't Hoff plots for guests **6d** and **9** were used to extract enthalpic and entropic effects, and values of ΔH and $-T\Delta S$ at 300 K are summarized in Figure 4. For guest **6d**, the entropic term is decreased by -4.1 kcal mol^{-1} in cavitand **5** compared to **3** as anticipated for the presence of covalent bridges, but an unfavorable increase of the enthalpic term of +3.6 kcal mol^{-1} was also observed in cavitand **5**. This may arise from deformations due to its covalent bridges that prevent the collapse of the cavitand walls for optimal cation- π interactions.¹³ Similar and more pronounced variations were noticed for the smaller guest **9** with a favorable decrease of the entropic term of -9.5 kcal mol^{-1} and a compensating unfavorable increase of the enthalpic term of +9.1 kcal mol^{-1} with cavitand **5** compared to **3**. The causes of these higher variations are less clear as the upfield regions of the ^1H NMR spectra of **9** with cavitands **3** and **5** show quite different patterns of signals for the bound guest.⁵ This points to different orientations of binding that annul direct comparisons. Nevertheless, for both guests, all of these variations lead only to a small decrease of ΔG in favor of **5**, which follows a trend frequently observed in entropy/enthalpy compensation phenomena.¹⁴

The activation barriers for dissociation of guests ΔG^\ddagger was also studied through EXSY experiments in $\text{DMSO-}d_6$ at 300 K for both **3** and **5** with guests **6d**, **8**, **9**, and **10** (Table 2). These barriers are consistently larger for **5** than **3**, ranging from +0.9 to +1.9 kcal mol^{-1} . The covalent connections in

(10) Biros, S. M.; Ullrich, E. C.; Hof, F.; Trembleau, L.; Rebek, J., Jr. *J. Am. Chem. Soc.* **2004**, *126*, 2870.

(11) Crampton, M. R.; Robotham, I. A. *J. Chem. Res., Synop.* **1997**, 22.

(12) Shivanyuk, A.; Friese, J. C.; Rebek, J., Jr. *Tetrahedron* **2003**, *59*, 7067.

(13) Cation- π interactions are known to depend on the distance between the cationic charge and the aromatic plane and also on the angle between the charge and the normal of the aromatic plane; see; Gilis, D.; Biot, C.; Buisine, E.; Dehouck, Y.; Rooman, M. *J. Chem. Inf. Model.* **2006**, *46*, 884.

(14) Gallicchio, E.; Kubo, M. M.; Levy, R. M. *J. Am. Chem. Soc.* **1998**, *120*, 4526.

Table 2. Activation Barriers for Dissociation of Both Cavitand Complexes at 300 K in DMSO-*d*₆ Obtained from EXSY Experiments and the Eyring Equation with *k*₋₁

guests	$\Delta G^{\ddagger a}$ (kcal mol ⁻¹)		$\Delta\Delta G^{\ddagger}$ (kcal mol ⁻¹) = $\Delta G^{\ddagger}(\mathbf{5}) - \Delta G^{\ddagger}(\mathbf{3})$
	3	5	
6d	16.9	18.8	+1.9
8	16.5	18.2	+1.8
9	16.2	17.3	+1.1
10	15.8	16.6	+0.9

^a Estimated error <0.1 kcal mol⁻¹.

5 must slow the unfolding of walls, a motion required to reach the dissociation transition state.

In conclusion, a new type of constrained extended cavitand has been synthesized via disulfide bond formation. The two

covalent bridges have only a small influence on the stability of the host–guest complexes but lead to more kinetic stability. Potential applications of this extended cavitand are underway and will be reported in due course.

Acknowledgment. We are grateful for financial support from the NIH (GM 27932) and the Skaggs Institute. E.B. is a Skaggs Post-Doctoral Fellow. We also thank Dr. Sacha Javor (Scripps Research Institute) for helpful discussions.

Supporting Information Available: Synthesis and characterization data for compound **2** and cavitands **3–5**, variable-temperature ¹H NMR spectra and van't Hoff plots, ROESY/NOESY spectra, EXSY calculations, and upfield regions of ¹H NMR spectra of both cavitands **3** and **5** with guests **6d** and **7–10**. This material is available free of charge via the Internet at <http://pubs.acs.org>.

OL101980F